Atmospheric Environment 57 (2012) 55–62

Contents lists available at SciVerse ScienceDirect

Atmospheric Environment

journal homepage: www.elsevier.com/locate/atmosenv

Intraseasonal variability of surface ozone in Santiago, Chile: Modulation by phase of the Madden–Julian Oscillation (MJO)

Bradford S. Barrett [a,*], Sean J. Fitzmaurice [b], Sarah R. Pritchard [a]

[a] Oceanography Department, U.S. Naval Academy, 572C Holloway Rd., Annapolis, MD 21401, USA
[b] Naval Nuclear Power Training Command, Charleston, SC, USA

HIGHLIGHTS

- Surface ozone concentration in Santiago, Chile varies intraseasonally by phase of the Madden–Julian Oscillation.
- Phase of the Madden–Julian Oscillation also affects the diurnal cycle of ozone concentration in Santiago.
- Days with low (high) ozone corresponded to days with anomalously high (low) cloud cover.

ARTICLE INFO

Article history:
Received 18 January 2012
Received in revised form
16 April 2012
Accepted 18 April 2012

Keywords:
Surface ozone
Intraseasonal
Santiago
Madden–Julian Oscillation

ABSTRACT

In Santiago, Chile, summertime surface ozone (O_3) concentrations regularly exceed local and international health thresholds due to high antecedent pollutants, frequent clear skies, and warm surface air temperatures. However, few (if any) studies exist that have examined the intraseasonal variability of surface O_3 or its modulation by phase of the Madden–Julian Oscillation (MJO). Therefore, the main objectives of this study were to investigate the intraseasonal variability of surface O_3 and the meteorological parameters known to affect O_3 concentrations during summer months in Santiago, and connect any observed variability to phase of the MJO. Ozone concentrations at seven stations in the Chilean National Air Quality Information System (SINCA), along with upper-air, surface, and reanalysis data, were used to create composites for each phase of the MJO. Results confirm that for the Santiago metropolitan region, both maximum daily O_3 concentrations, as well as the diurnal cycle of O_3, depend on MJO Phase. Ozone concentrations were highest during Phases 5 and 6 and lowest during Phases 1 and 2. Cloud cover anomalies best agreed with this pattern of O_3 variability, with low (high) cloud cover anomalies occurring during days with high (low) ozone. Surface temperature and strength and height of the lower-troposphere temperature inversion had similar, but less pronounced, connections to O_3, with slightly warmer surface temperatures and stronger inversions closer to the ground occurring on days with higher O_3. Wind velocity was found to vary little between days with low and high ozone.

Published by Elsevier Ltd.

1. Introduction

Ozone (O_3) is one of the most important trace gasses in the troposphere. As a secondary pollutant, its concentrations are controlled by complex processes involving anthropogenic emissions, chemical reactions between primary pollutants and ultraviolet solar radiation, and meteorology. It strongly affects human health, vegetation, and ecosystems in industrial, suburban, and rural areas worldwide and is expected to increase significantly during the 21st century. In Santiago, Chile, maximum hourly O_3 concentrations regularly reach between 100 and 150 parts per billion by volume (ppbv) in summer, occasionally peaking above 320 ppbv in the eastern (downwind) part of the city (Gramsch et al., 2006), well in excess of Chilean (0.075 ppmv hourly maximum) and U.S. (0.08 ppmv 8-h concentration) health thresholds. Ozone exposure at these levels produces harmful structural changes in human cells, specifically lesions in the centriacinar area of the lungs at the ends of the terminal bronchioles (Lippmann, 1989; Burnett et al., 1997). These effects cause respiratory problems, especially in those with chronic lung diseases, and can seriously damage the lining of the lung when inhaled over a long-period of time (Sanhueza et al., 2003). Even short-term (daily and weekly) exposure to ambient tropospheric O_3 has been associated with adverse effects on public health and increased mortality (Bell et al., 2004). For all these reasons, studies that determine the behavior of O_3 across a range of temporal and spatial scales are important.

* Corresponding author. Tel.: +1 410 293 6567; fax: +1 410 293 2137.
E-mail address: bbarrett@usna.edu (B.S. Barrett).

1352-2310/$ – see front matter Published by Elsevier Ltd.
doi:10.1016/j.atmosenv.2012.04.040

However, intraseasonal variability of ground-level O_3 has yet to be comprehensively examined. Therefore, the main objectives of this study were to (1) investigate the intraseasonal variability of surface O_3 and related meteorological parameters during summer months in Santiago, Chile, and (2) connect any observed variability to phase of the leading mode of atmospheric intraseasonal variability, the Madden–Julian Oscillation (MJO; Madden and Julian, 1971).

The MJO manifests itself as a large-scale convective anomaly over the maritime continent. Its most basic feature consists of an eastward moving region of deep convective clouds and heavy precipitation bounded on both the west and east by regions of suppressed convection and minimal precipitation. Zonal circulations connect the two regions, with lower-troposphere (near 850-hPa) anomalous westerly (easterly) winds to the west (east) of the deep convection; in the upper troposphere (near 200-hPa), the circulation anomalies reverse (Madden and Julian, 1972). The convective anomalies have been observed to remain between the Indian Ocean and 180°, while the circulation anomalies have been observed to circumnavigate the tropics.

The oscillation has significant interaction with the extratropics, including teleconnections to the Western Hemisphere. Modeling studies of Berbery et al. (1992) and Mechoso et al. (1991), as well as the theoretical findings of Hoskins and Karoly (1981) and Bladé and Hartmann (1995), confirmed that the MJO modulates Rossby wave activity. Sardeshmukh and Hoskins (1988) found a pathway to the extratropics in both hemispheres, noting that a divergence field in easterly flow asymmetric about the Equator (a consequence of deep convection) led to an extremely effective Rossby wave source in the subtropical westerlies. Barrett et al. 2012 used this pathway to explain modulation of winter precipitation in Chile by phase of the MJO. A similar technique was used for this study to explain the link between intraseasonal ground-level O_3 variability in Santiago and the MJO. Detailed reviews of the MJO are presented in Madden and Julian (1994), Lau and Waliser (2005), and Zhang (2005).

During austral summer, central Chile frequently experiences clear skies and high temperatures due to the presence of the subtropical anticyclone centered in the southeast Pacific Ocean (Schmitz, 2005; Rutllant and Garreaud 2004; Garreaud and Muñoz, 2005). Additionally, because of a persistent low-level inversion and its orographic location at the rim of the highest peaks of the Andes Mountains, Santiago is a poorly ventilated location. Furthermore, low morning mixing heights, a result of the presence of a coastal trough immediately west of central Chile, often result in above normal afternoon surface temperatures, reaching between 30° and 35 °C in Santiago (Rappenglück et al., 2000). Surface O_3 production under these conditions is favored, as the photochemical oxidation of carbon monoxide (CO) and volatile organic compounds (VOC) occurs in the presence of high concentrations of nitrogen oxides (NO and NO_2; Rappenglück et al., 2000, 2005; Elshorbany et al., 2009a, b).

The most important factor determining surface O_3 concentrations in Santiago is the amount of insolation received, as evidenced by the pronounced daily and seasonal O_3 cycles (e.g., Gramsch et al., 2006; Schmitz, 2005). On the daily cycle, surface O_3 concentrations reach a minimum of 0–5 ppbv at daybreak (0600 local time, hereafter LT) and quickly build during the day, peaking around 1400 LT and then declining again in the evening hours (Elshorbany et al., 2009a; Villena et al., 2011). On the seasonal cycle, O_3 concentrations reach a winter minimum (mean daily values less than 20 ppbv) in June and then build to a summer maximum (mean daily greater than 70 ppbv) between December and March (Gramsch et al., 2006; Elshorbany et al., 2010). Besides the relationship to insolation, other meteorological factors have also been suggested to affect O_3 concentrations in Santiago. For example, Rubio et al. (2004) found a positive linear association between maximum O_3 levels and maximum local temperature at Las Condes, with ozone exceeding 80 ppbv on 87% of days with temperature above 29 °C but exceeding 80 ppbv on only 16% of days where the temperature did not exceed 29 °C. They speculated that the relationship would be similar across other sites in the city. Rubio et al. (2004) also found that the VOC/NO_x ratio (and thus surface O_3 concentrations) increased during days with high surface temperature because of an increase in hydrocarbon evaporation and biogenic emissions. Additionally, the diurnal O_3 shoulder (slower rate of decline in afternoon O_3) has been explained by the favorable predominant afternoon wind direction from the southwest carrying biogenic emissions to the city center (Gramsch et al., 2006). In this study, we will examine these meteorological parameters as they relate to surface O_3 variability on the intraseasonal time scale. The remainder of the paper is organized as follows: data and methodology are described in Section 2; intraseasonal variability of O_3 and meteorological factors affecting the observed O_3 variability are presented in Section 3; and a discussion and conclusions are presented in Section 4.

2. Data and methods

Santiago, Chile, a city with a population of around 6 million, lies in a slightly sloped valley, with a mean elevation of 500 m that rises gradually from its low point in the west to its high point in the east. Further to the east of Santiago rises the Andes Cordillera, with peaks reaching 5500 m. A lower coastal range is located to the west of Santiago with elevations up to 2000 m. Hourly O_3 concentration data in ppbv were collected at three observing stations located in the central and eastern side of Santiago (Las Condes, Parque O'Higgins, and Independencia) during the summer months of November–February from Jan 1988–Dec 2010. Four additional stations in Santiago with data records from Jan 1997–Dec 2010 were also examined. Besides O_3, all seven of the stations also measured hourly surface wind velocity from Jan 2004–Dec 2011. All data are available publicly from the National Air Quality Information System (SINCA, http://sinca.conama.cl), operated by the Ministry of the Environment. Table 1 summarizes the ozone concentration measurements and Fig. 1 shows the topography of Santiago and the locations of the observing stations; see Gramsch et al. (2006) for a detailed description of each station, including a description of surrounding buildings, roads, and parks.

Phase of the MJO was determined using the Real-time Multivariate MJO Index (RMM; Wheeler and Hendon, 2004; hereafter WH04). The RMM is based on a pair of principal component time series derived from empirical orthogonal functions of near-equatorially averaged outgoing longwave radiation, 200-hPa zonal wind, and 850-hPa zonal wind. The projection of daily data onto the empirical orthogonal functions acts as an effective time filter and makes the index useful in a real-time setting (WH04). The RMM is divided into eight phases, each corresponding to a broad location of the MJO enhanced convective signal. Active MJO for this study was defined as one where the root sum of the two squared principal components, RMM1 and RMM2, was greater than one. It

Table 1
Ozone concentration descriptive statistics at each measuring station. Number of observations (n), mean, median, standard deviation, max, and min (in ppbv) of maximum daily concentrations.

Site	n	Mean	Median	Standard deviation	Max	Min
Las Condes	3449	70.9	69.5	44.8	475	0
Independencia	3522	48.7	46.1	32.0	364	0.048
Parque O'Higgins	3383	47.0	46.1	26.0	316	0.351

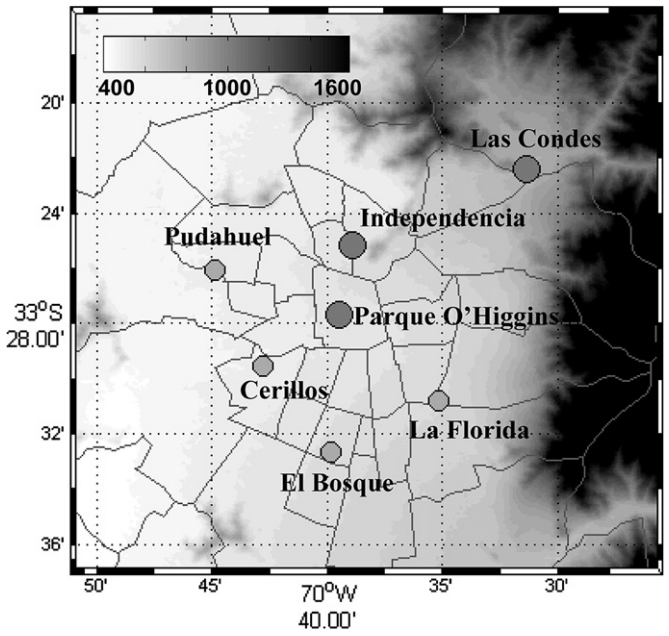

Fig. 1. Elevation (shaded contours, every 40 m from 400 m to 1600 m) and SINCA station locations (circles). Stations identified by larger circles have data from 1988 to 2010; those at smaller circles have data from 1997 to 2010. Communa political boundaries are in light gray.

is important to note that regional and national forecast centers are currently producing operational and ensemble predictions of the WH04 RMM Index (Jones et al., 2004; Wang, 2011), thus increasing the usefulness of statistical studies such as this one in the arena of intraseasonal prediction. A thorough description of the RMM Index and several examples showing how it can be used to diagnose MJO modulation of the atmosphere can be found in WH04, and the real-time RMM Index can be downloaded from http://cawcr.gov.au/staff/mwheeler/maproom/RMM/.

Following the technique outlined in Barrett et al. 2012, daily composites of maximum O_3 and the following meteorological variables were made for each MJO Phase: (a) total column cloud cover at 18Z (1400 LT), sea level pressure, and surface wind over Chile and the southeast Pacific Ocean (from NCEP/NCAR Reanalysis II; Kanamitsu et al., 2002), (b) air temperature, dew point temperature, cloud ceiling height, sea level pressure, and surface wind speed at Santiago International Airport (SCEL; from NCEP Global Summary of the Day), (c) afternoon wind speed and direction at the seven SINCA stations, and (d) 12Z upper-air data from Santo Domingo (SCSN) upper-air station (from the NCEP Integrated Global Radiosonde Archive, IGRA). Datasets (a) and (b) used daily data from Jan 1988–Dec 2010; dataset (c) used daily data from Jan 2004–Dec 2011; and dataset (d) used daily data from Feb 2002–Jan 2011. For each dataset, the longest possible record was used in an attempt to capture as many cycles of the MJO as possible. Data were checked for quality, and bad or missing data were excluded from the analysis. For surface data, wind directions of 999 were removed, wind speeds above 50 m s^{-1} removed, temperatures above 50 °C removed, dew point temperatures above 30 °C removed, sea level pressures above 1050 mb removed, and ceiling heights above 22,000 m removed. For upper-air data, temperature changes greater than 30 °C were removed. Finally, it is important to note that while total cloud fraction is a "Class C" variable in Reanalysis and has known biases (e.g., Clark and Walsh, 2010), the benefits of a consistent, long-period record support its inclusion in this study.

Mean temperature and pressure of the lower-tropospheric inversion were calculated from upper-air observations at SCSN. For each 12Z (0800 LT) sounding, temperature data below 700 hPa was iteratively searched to first identify if a local inversion existed. If one did exist, the data were searched a second, third, and sometimes fourth time to determine whether other inversions existed. If any inversions were found, the inversion with the greatest temperature increase was selected. Inversion temperature change was measured from the point where temperature began to increase to where it began decreasing again, and this temperature change, along with the pressure level of the warmest temperature of the inversion, were used to create the composites.

3. Results

Maximum daily O_3 concentrations at Las Condes, Independencia, and Parque O'Higgins (see Fig. 1 for station locations and Table 1 for a summary of descriptive statistics) all showed a distinct pattern of variability with phase of the MJO (Fig. 2). On days when the MJO Index was in Phases 5, 6, and 7, O_3 concentrations were high, while on days when the index was in Phases 8, 1, and 2, O_3 concentrations were low. Furthermore, the differences in concentrations between Phases 1 and 6 (Phases 1 and 5 at Independencia) were statistically significant at the 95% confidence level for all three stations using the Student's *t*-test. While the number of daily observations in each binned phase varied for the three stations, each phase was comprised of between 290 and 375 observations.

Hourly O_3 concentrations at each station also showed distinct variability with phase of the MJO (Fig. 3). Ozone concentrations peaked around 1400 LT, with the highest hourly O_3 occurring on days when the MJO Index was in Phase 6. Lowest maximum O_3 also peaked around 1400 LT and occurred on days when the MJO Index was in Phase 1. This result agrees well with the maximum daily concentrations in Fig. 2. All three stations exhibited the same diurnal cycle, with O_3 reaching a minimum background value close to 5 ppbv around 0500 LT, increasing rapidly during the morning to peak at around 1400 LT, then decreasing again in the afternoon with a rapid decline after sunset. The afternoon O_3 shoulder, noted by other authors (e.g., Elshorbany et al., 2009b), was visible at both Independencia and Parque O'Higgins, and the hourly O_3 values in the shoulder mirror those at the peak: highest O_3 during Phase 6, lowest during Phase 1. The shape of the shoulder was the same for all MJO phases.

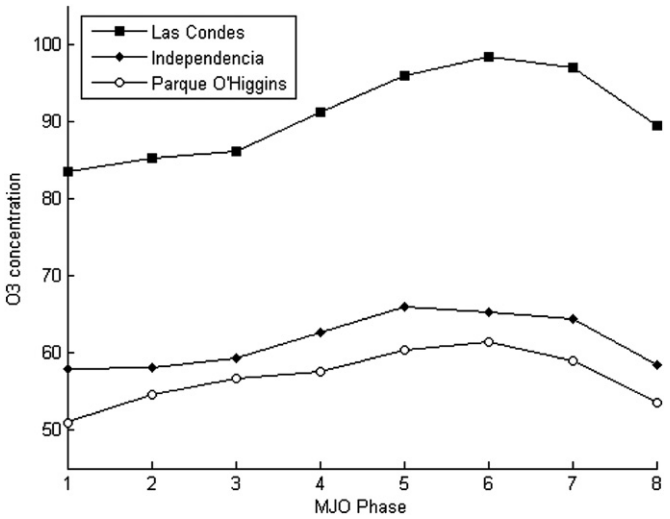

Fig. 2. Average maximum daily ozone concentrations by MJO Phase (concentrations in parts per billion, by volume).

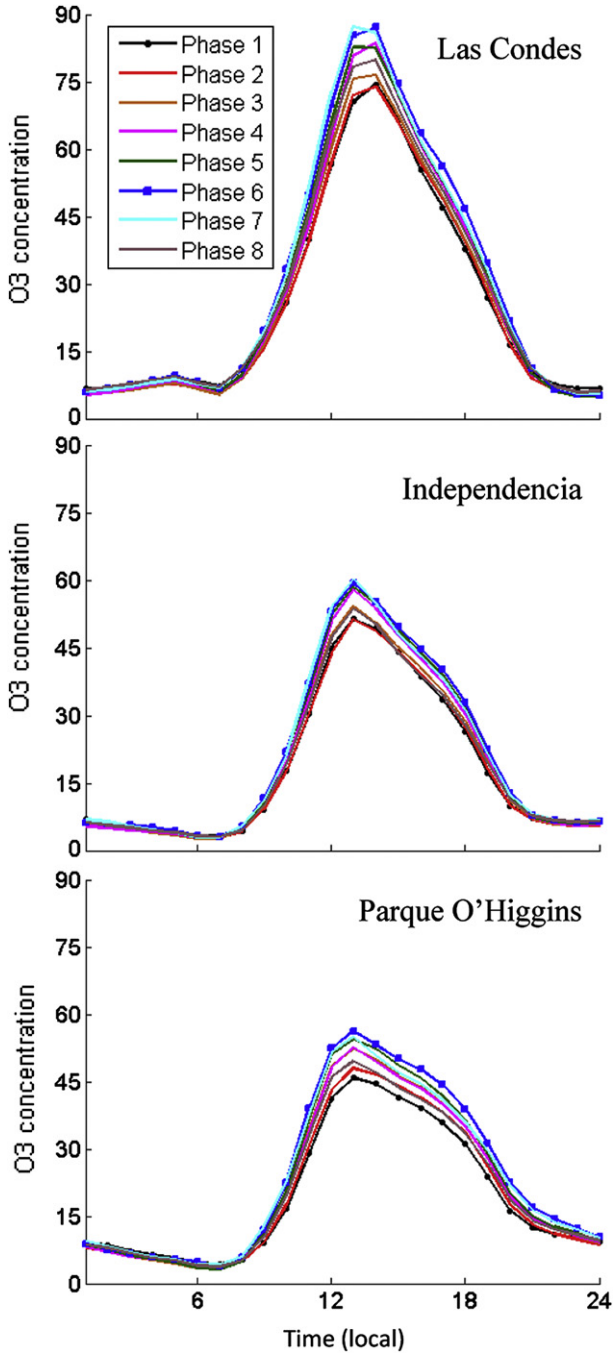

Fig. 3. Diurnal cycle of ozone concentration (ppbv) at Las Condes, Independencia, and Parque O'Higgins, 1988–2010, by MJO Phase. Phases 1 and 6 indicated by circles and squares, respectively.

Previous authors studying summer O_3 in Santiago have found that its concentrations are linked to different meteorological variables, including insolation, surface wind, mixing, surface temperature, and surface dew point temperature. We examined these in turn to test their relationship to intraseasonal O_3 variability. The first meteorological variable examined was total cloud cover, which was used as a proxy for insolation. Cloud cover anomalies agreed well with the observed ozone-MJO variability: during MJO Phases 8, 1, and 2, cloud cover was anomalously high, while during MJO Phases 5 and 6, cloud cover was anomalously low (Fig. 4). Considering that normal summer insolation is already high in Santiago, anomalously low (high) cloud cover would thus allow more (less) ultraviolet radiation to reach the surface and allow more (fewer) ozone-producing photochemical reactions. Of the meteorological variables examined in this study, cloud cover anomalies agreed best with the O_3 observations.

The second meteorological parameter examined, sea level pressure anomalies, also exhibited significant variability by MJO Phase. Low (high) sea level pressure anomalies were centered about 2000 km southwest of Santiago near 45°S, 90°W during MJO Phase 1 (Phase 6; see Fig. 5). Similarly, weak high (low) sea level pressure anomalies were centered along the central and north-central Chilean coast during Phase 1 (Phase 6). Corresponding surface wind anomalies accompanied the sea level pressure anomalies, with northerly surface wind anomalies occurring during Phase 1 and southerly anomalies during Phase 6. Both the sea level pressure and surface wind anomalies agreed well with the phases of lowest and highest surface O_3, with the lowest O_3 occurring during Phase 1 and highest during Phase 6.

Next, tropospheric temperatures were examined along a cross-section at 33°S, the latitude of Santiago. Temperature anomalies also varied by MJO Phase, with the strongest contrast in lower-troposphere (surface to 700 hPa) temperatures found between Phases 1 and 6 (Fig. 6). For days when the MJO Index was in Phase 1 (during which O_3 was lowest), neutral surface temperatures near and west of Santiago (from 70°W to 75°W) turned to cold anomalies near 850 hPa. The pattern reversed on days when the MJO Index was in Phase 6 (during which O_3 was highest), with warm surface temperatures transitioning to even warmer temperature anomalies near 850 hPa. Cold temperature anomalies throughout the lower-troposphere were observed in Phases 2 and 3, and warm anomalies were observed in Phases 7 and 8. These anomalies mapped onto the existing thermal profile of central Chile, which is often characterized by a lower-troposphere morning temperature inversion (Garreaud and Muñoz, 2005).

The vertical profiles of temperature (Fig. 6) suggested weaker temperature inversions on days when the MJO Index was in Phase 1 and stronger temperature inversions on days when the index was in Phase 6. To test this hypothesis, 12Z sounding data were examined from the regular upper-air station at Santo Domingo (along the coast approximately 90 km west-southwest of Santiago). During Phases 1 and 2, inversion strength (measured by the change in temperature from the base to the top of the inversion) was lowest, around 5–5.5 °C (Fig. 7). During Phases 6, 7, and 8, inversion strength was highest, between 7 and 7.5 °C. Inversion pressure levels (the pressure level of the base of the inversion) were highest (farthest from the ground) during Phases 7, 8, 1, and 2 and lowest (closest to the ground) during Phases 3, 4, and 5. These data were roughly in agreement with the temperature cross-sections, and indicated that MJO Phases with colder (warmer) lower-troposphere temperatures and weaker (stronger) low-level temperature inversions roughly corresponded to MJO Phases with lower (higher) surface O_3. These differences between phases, however, were not statistically significant at the 95% confidence level.

In addition to the radiosonde data, morning, noon, and afternoon (0600, 1200, and 1800 LT) surface conditions at the Santiago International Airport (SCEL) were also examined. Greatest variability by phase of the MJO was found in sea level pressure, with low sea level pressures occurring during Phases 5, 6, and 7 and high pressures during Phases 1 and 2 (Fig. 8), in good agreement with the reanalysis sea level pressure pattern (Fig. 5). The variability in sea level pressure, along with the cloud cover anomalies in Fig. 4, agree with the findings of Rutllant and Garreaud (1995), who noted that clear skies in central Chile were most often associated with a coastal pressure trough. Furthermore, the difference in sea level pressure between Phases 2 and 6 was statistically significant at the

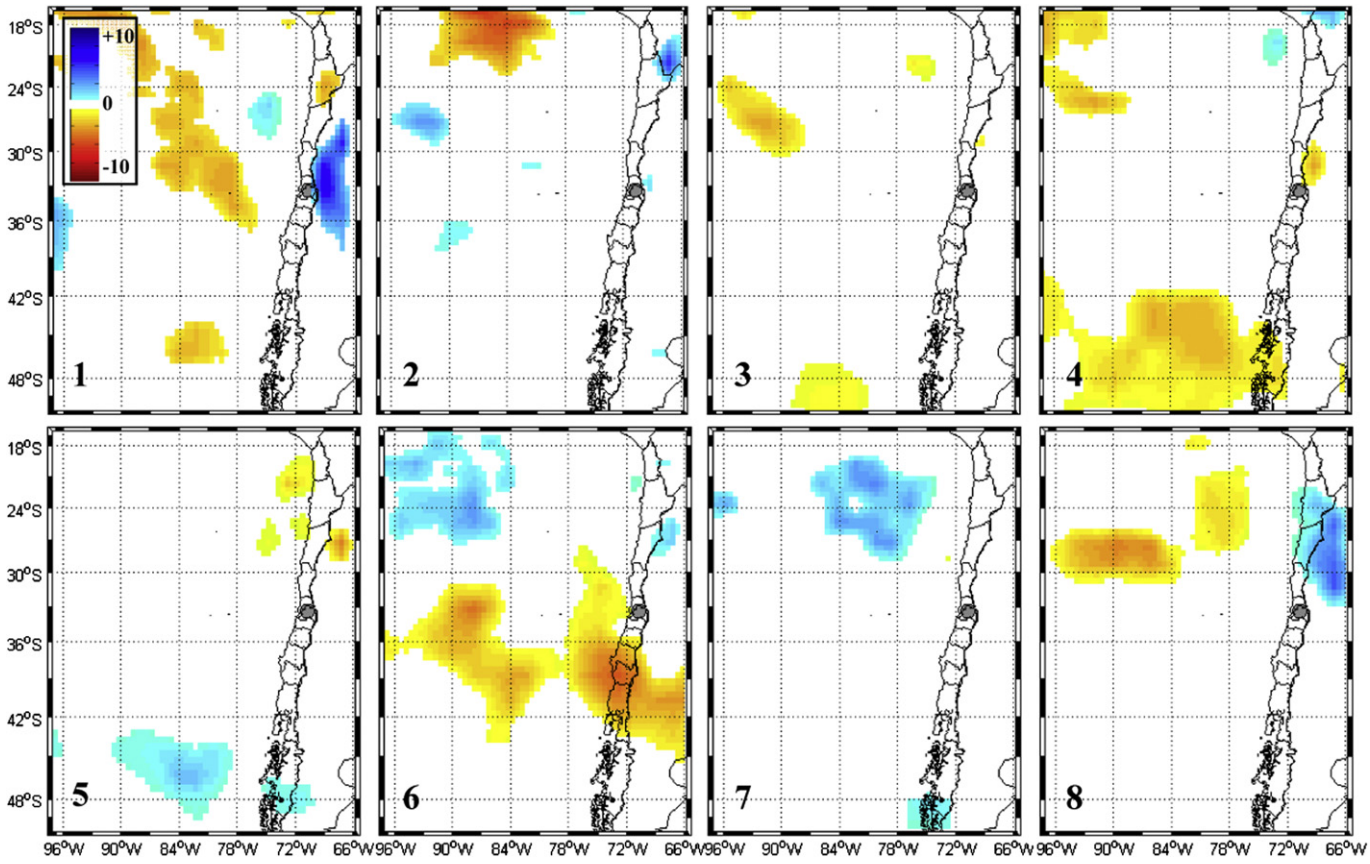

Fig. 4. Total cloud fraction anomaly (units in % cloud fraction) by MJO Phase. Only anomalies that are statistically significant at the 95% confidence level shown. Phase number noted in lower-left, Santiago indicated by a gray circle, and black lines indicate political boundaries. Contour interval is every 0.25% cloud fraction.

95% confidence level. Morning, noon, and afternoon cloud ceiling heights, which we considered as another approximation for insolation, were highest during Phases 5 and 6, and lowest during Phases 8, 1, and 2, again in rough agreement with the phases with high (Phases 5 and 6) and low (Phases 1 and 2) O_3.

Not all of the meteorological parameters at SCEL showed as much variability between MJO Phases as cloud cover, sea level pressure, and ceiling height. Noon and afternoon surface temperature anomalies, which were lowest during Phases 1 and 2, were only neutral to slightly positive during MJO Phases 5 and 6 and highest in Phases 7 and 8. Noon dew point temperature anomalies were lowest in Phases 5 and 6 and highest in Phases 8, 1, and 2; however, the anomalies were not large. Wind speed anomalies, noted in earlier studies as possibly being responsible for the afternoon O_3 shoulder at Parque O'Higgins and Independencia, were highest in Phases 8 and 1, neutral in Phases 5 and 6, and lowest in Phase 4. However, wind velocity, both speed and direction, at each SINCA station did not change significantly between MJO Phases 1 and 6 (Fig. 9).

4. Discussion and conclusions

Surface ozone has been the subject of many studies in Santiago and other global cities. However, few (if any) studies exist that have examined its intraseasonal variability or connection to phase of the MJO. The results presented here confirm that for the Santiago metropolitan region, both maximum daily O_3 concentrations as well as the diurnal cycle of O_3 varied by MJO Phase, with lowest O_3 occurring on days with the MJO Index in Phases 1 and 2 and highest O_3 occurring on days with the MJO Index in Phases 5 and 6. Additionally, the difference between the lowest (Phase 1) and highest (Phase 6) concentrations was statistically significant at the 95% confidence level. Composite anomalies of total cloud cover were in good agreement with the O_3 data, with highest (lowest) cloud cover anomalies occurring in the phases with lowest (highest) surface O_3 concentrations. Sea level pressure and surface wind anomalies provided supporting evidence for a meteorological explanation for the observed O_3 anomalies, with a surface pressure trough (ridge) located along the Chilean coast during phases of high (low) cloud cover and O_3. Surface data at Santiago International Airport varied by phase of the MJO, with highest (lowest) surface pressures occurring during periods of low (high) O_3, a result that is statistically significant at the 95% confidence level. These results are both in good agreement with each another, suggesting that anomalously low sea level pressures and clear skies are associated with higher O_3 concentrations.

Surface temperature and ceiling height were somewhat in agreement with O_3 concentrations, with higher (lower) temperature and ceiling anomalies mostly occurring during phases with high (low) O_3 concentrations, but the variability was not statistically significant. Wind velocities over Santiago showed little change between Phases 1 and 6. Lower-tropospheric temperature anomalies over and upstream of Santiago were found to reverse signs, depending on MJO Phase: cold anomalies occurred during Phase 1, warm anomalies occurred during Phase 6, suggesting a modulation of the temperature inversion by the MJO. Indeed, data from the nearest regular upper-air station show weaker (stronger) and higher (lower) above-ground temperature inversions during the low (high) ozone phases, although like the surface data from the airport, the signal was not as pronounced as that found in either

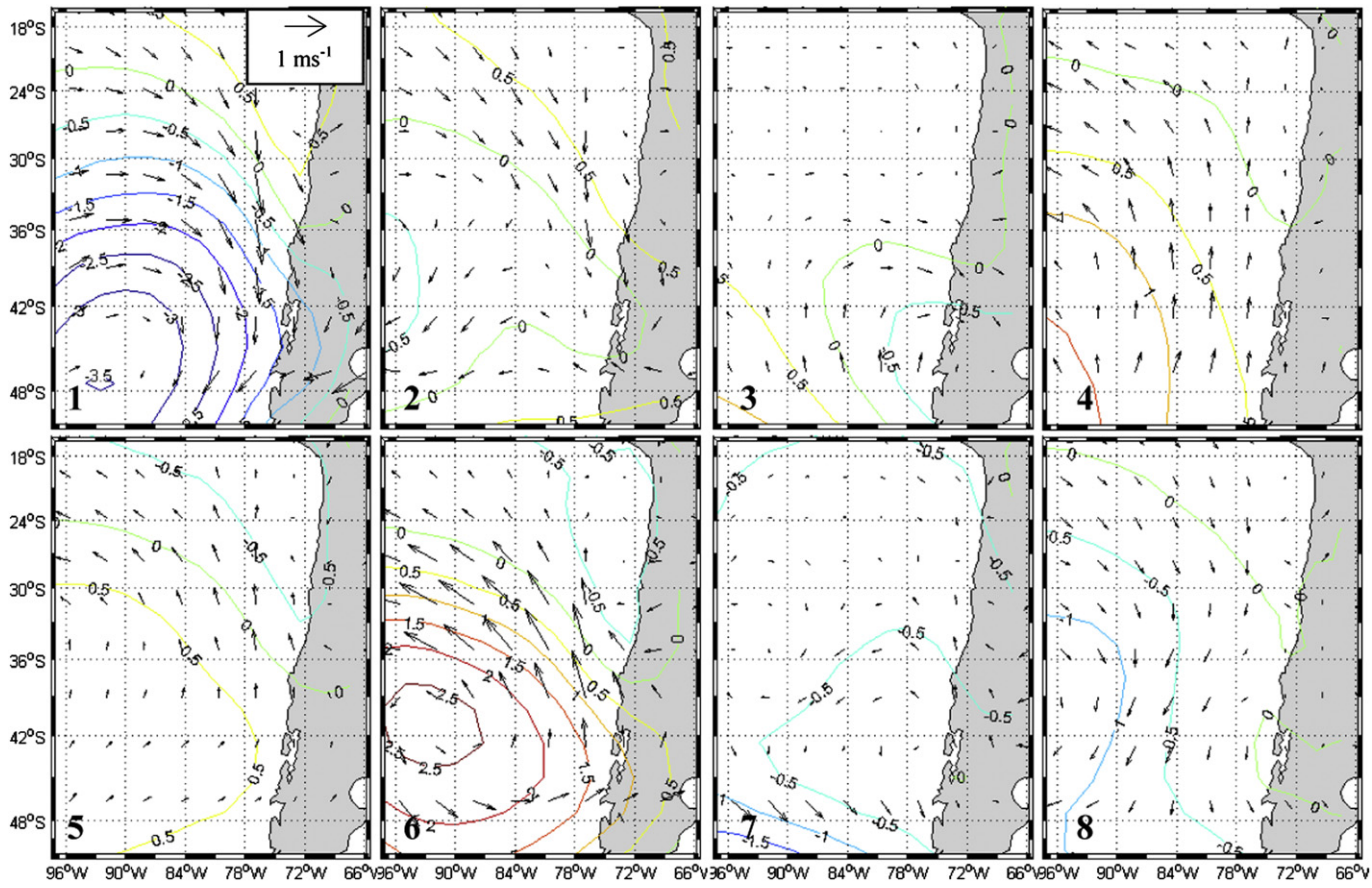

Fig. 5. Summer surface wind and sea level pressure anomalies (in mb), by MJO Phase.

cloud cover anomalies or sea level pressure. These results agree with Berman et al. (1999), who suggested that a relationship existed between morning inversion height and strength and summer O_3 in Houston. However, the relationship between surface O_3 and low-level temperature inversions remains unclear, as Rappenglück et al. (2008) found essentially the opposite result, and Banta et al. (2011) found that neither boundary layer depth nor maximum surface temperature affected surface O_3 in Houston, but rather lower-troposphere wind direction.

For Santiago, we found the greatest intraseasonal relationship between O_3 and cloud cover, with secondary agreement with surface and lower-troposphere temperature. Because cloud cover

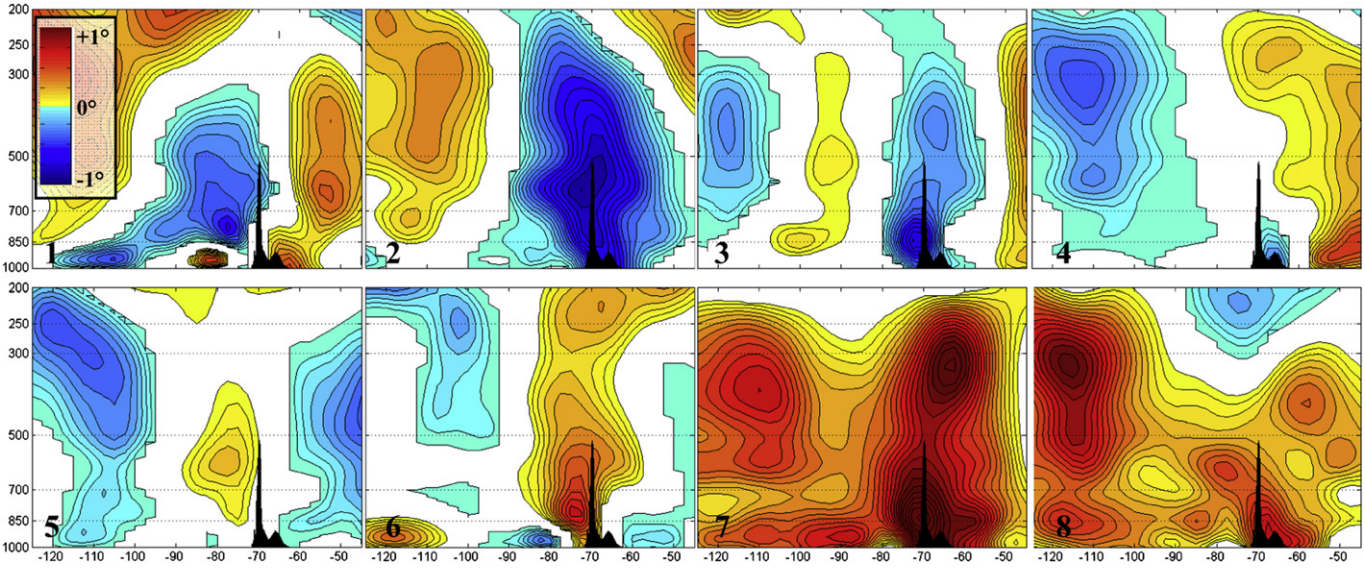

Fig. 6. Summer tropospheric temperature anomalies in °C along 33°S, by MJO Phase. Black shading indicates topography, and phase number indicated in lower-left of each panel.

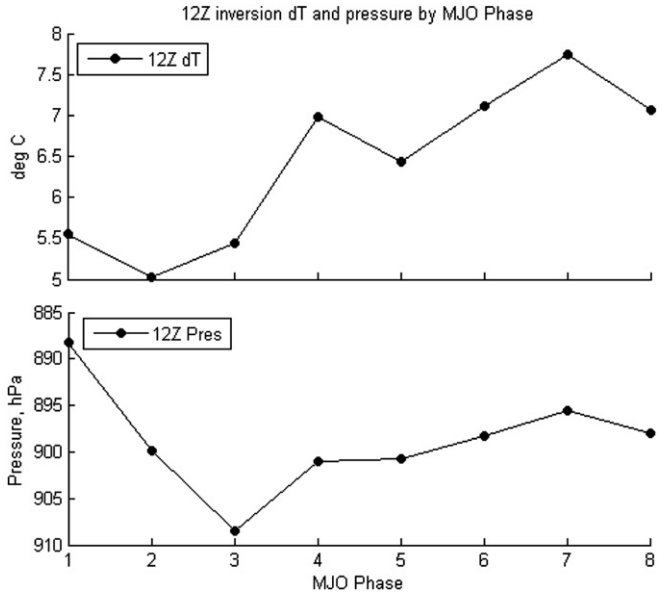

Fig. 7. Summer inversion temperature change (dT, in °C) and pressure (in hPa) by MJO Phase at SCSN (Santo Domingo) upper-air station, 2002–2011.

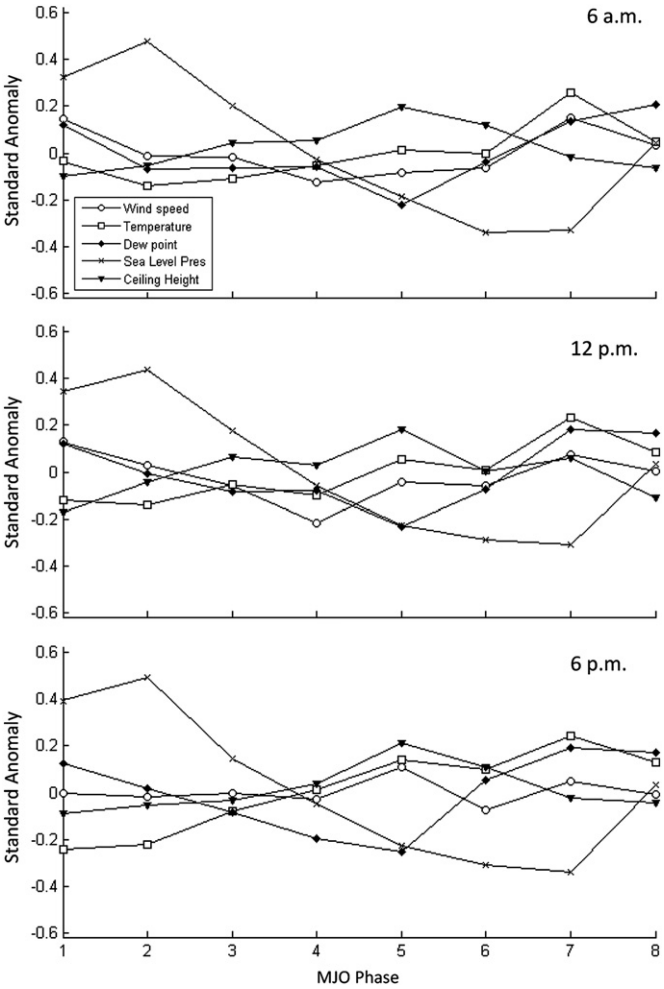

Fig. 8. Standardized anomalies of state variables at SCEL (Santiago international airport) by MJO Phase, summers 1988–2010.

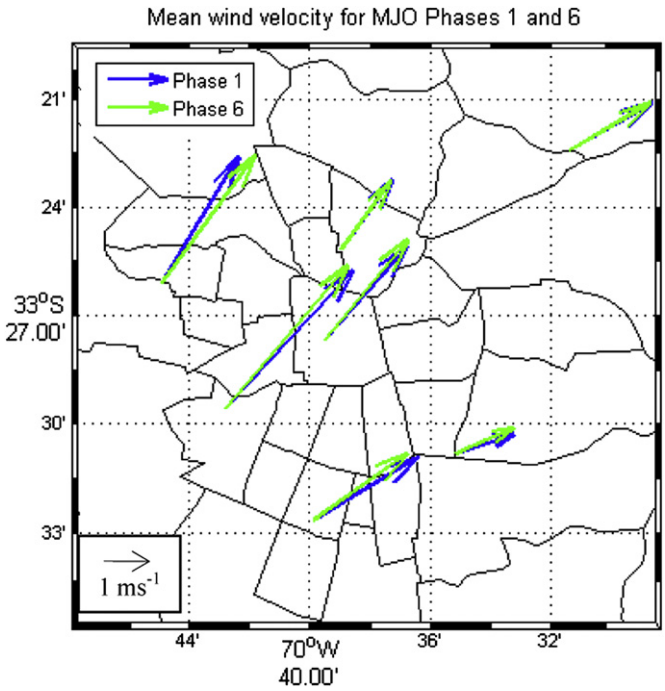

Fig. 9. Mean wind velocities for MJO Phase 1 (low ozone) and Phase 6 (high ozone). Communa political boundaries are outlined in black.

in Santiago is often related to the strength and height of the lower-troposphere temperature inversion (e.g., Rutllant and Garreaud, 1995), the amount of influence that inversion strength and height would have on O_3 would depend on how much the inversion affected insolation and diurnal mixing of morning stratus. In this study, those variables were not examined in depth due to lack of upper-air observations over Santiago. Also, it is important to note that the radiosonde data used in this study were collected at sea level along the coast 90 km west-southwest of Santiago, thereby sampling a more marine environment than that characteristic of Santiago. Thus, additional research – particularly research that incorporates upper-air information from the air column above Santiago – is needed to further solidify the relationship between the lower-tropospheric temperature and surface O_3.

Finally, it is important to note that O_3 variability by MJO Phase for the other four SINCA stations (with data from 1997 to 2010) resembled the pattern in Fig. 3 for MJO Phases 1 to 7. However, O_3 concentrations in Phase 8 behaved differently from those at Las Condes, Independencia, and Parque O'Higgins, increasing during Phase 8 rather than decreasing. Additionally, when the 1997–2010 record was isolated for all seven stations, the anomalous increase at Phase 8 was seen at all locations. While several factors may explain this anomaly, including lack of sufficiently long data records to capture multiple cycles of the MJO, additional research is needed to determine whether a material change in the relationship to the MJO has occurred for Phase 8 in recent years.

Acknowledgments

We would like to thank the U.S. Naval Academy Research Council (NARC) for financial support for this investigation. Additionally, NCEP Reanalysis 2 data was provided by the NOAA/OAR/ESRL PSD, Boulder, Colorado, USA, from their Web site at http://www.esrl.noaa.gov/psd/. We also thank two anonymous reviewers for their helpful comments to improve the manuscript.

References

Banta, R.M., Senff, C.J., Alvarez, R.J., Langford, A.O., Parrish, D.D., Trainer, M.K., Darby, L.S., Hardesty, R.M., Lambeth, B., Neuman, J.A., Angevine, W.M., Neilsen-Gammon, J., Sandberg, S.P., White, A.B., 2011. Dependence of daily peak O_3 concentrations near Houston, Texas on environmental factors: wind speed, temperature, and boundary-layer depth. Atmospheric Environment 45, 162–173.

Barrett, B.S., Carrasco, J.F., Testino, A.P., 2012. Madden-Julian Oscillation (MJO) modulation of atmospheric circulation and Chilean winter precipitation. Journal of Climate 25, 1678–1688.

Bell, M., McDermott, A., Zeger, S., Samet, J., Dominici, F., 2004. Ozone and short-term mortality in 95 US urban communities, 1987–2000. Journal of the American Medical Association 292, 2372–2378.

Berbery, E.H., Nogués-Paegle, J., Horel, J.D., 1992. Wavelike southern hemisphere extratropical teleconnections. Journal of the Atmospheric Sciences 49, 155–177.

Berman, S., Jia-Yeong, K., Trivikrama Rao, S., 1999. Spatial and temporal variation in the mixing depth over the northeastern United States during the summer of 1995. Journal of Applied Meteorology 38, 1661–1673.

Bladé, I., Hartmann, D.L., 1995. The linear and nonlinear extratropical response of the atmosphere to tropical intraseasonal heating. The Journal of Atmospheric Science 52, 4448–4471.

Burnett, R.T., Brook, J.R., Yung, W.T., Dales, R.E., Krewski, D., 1997. Association between ozone and hospitalization for respiratory diseases in 16 Canadian cities. Environmental Research 72, 24–31.

Clark, J.V., Walsh, J.E., 2010. Observed and reanalysis cloud fraction. Journal of Geophysical Research 115, D23121.

Elshorbany, Y.F., Kleffmann, J., Kurtenbach, R., Rubio, M., Lissi, E., Villena, G., Gramsch, E., Rickard, A.R., Pilling, M.J., Wiesen, P., 2009a. Summertime photochemical ozone formation in Santiago, Chile. Atmospheric Environment 43, 6398–6407.

Elshorbany, Y.F., Kurtenbach, R., Wiesen, P., Lissi, E., Rubio, M., Villena, G., Gramsch, E., Rickard, A.R., Pilling, M.J., Kleffmann, J., 2009b. Oxidation capacity of the city air of Santiago, Chile. Atmospheric Chemistry and Physics 9, 2257–2273.

Elshorbany, Y.F., Kleffmann, J., Kurtenbach, R., Lissi, E., Rubio, M., Villena, G., Gramsch, E., Rickard, A.R., Pilling, M.J., Wiesen, P., 2010. Seasonal dependence of the oxidation capacity of the city of Santiago de Chile. Atmospheric Environment 44, 5383–5394.

Garreaud, R.D., Muñoz, R.C., 2005. The low-level jet off the west coast of subtropical South America: structure and variability. Monthly Weather Review 133, 2246–2261.

Gramsch, E., Cereceda-Balic, F., Oyola, P., von Baer, O., 2006. Examination of pollution trends in Santiago de Chile with cluster analysis of PM_{10} and ozone data. Atmospheric Environment 40, 5464–5475.

Hoskins, B.J., Karoly, D.J., 1981. The steady linear response of a spherical atmosphere to thermal and orographic forcing. Journal of the Atmospheric Sciences 38, 1179–1196.

Jones, C., Carvalho, L.M.V., Higgins, W., Waliser, D., Schemm, J.-K., 2004. A statistical forecast model of tropical intraseasonal convective anomalies. Journal of Climate 17, 2078–2095.

Kanamitsu, M., Ebisuzaki, W., Woollen, J., Yang, S.-K., Hnilo, J.J., Fiorino, M., Potter, G.L., 2002. NCEP-DOE AMIP-II reanalysis (R-2). Bulletin of American Meteorological Society 83, 1631–1643.

Lau, W.K.M., Waliser, D.E., 2005. Intraseasonal Variability of the Atmosphere-ocean Climate System. Springer, Heidelberg, Germany, 474 pp.

Lippmann, M., 1989. Health effects of ozone: a critical review. Journal of the Air Pollution Control Association 39, 672–695.

Madden, R.A., Julian, P.R., 1971. Detection of a 40–50 day oscillation in the zonal wind in the tropical Pacific. Journal of the Atmospheric Sciences 28, 702–708.

Madden, R.A., Julian, P.R., 1972. Description of global-scale circulation cells in the tropics with a 40–50 day period. Journal of the Atmospheric Sciences 29, 1109–1123.

Madden, R.A., Julian, P.R., 1994. Observations of the 40–50 day tropical oscillation: a review. Monthly Weather Review 122, 814–837.

Mechoso, C.R., Farrara, J.D., Ghil, M., 1991. Intraseasonal variability of the winter circulation in the southern hemisphere atmosphere. Journal of the Atmospheric Sciences 48, 1387–1404.

Rappenglück, B., Oyola, P., Olaeta, I., Fabian, P., 2000. The evolution of photochemical smog in the metropolitan area of Santiago de Chile. Journal of Applied Meteorology 39, 275–290.

Rappenglück, B., Schmitz, R., Bauerfeind, M., Cereceda-Balic, F., von Baer, D., Jorquera, H., Silva, Y., Oyola, P., 2005. An urban photochemistry study in Santiago de Chile. Atmospheric Environment 39, 2913–2931.

Rappenglück, B., Perna, R., Zhong, S., Morris, G.A., 2008. An analysis of the vertical structure of the atmosphere and the upper-level meteorology and their impact on surface ozone levels in Houston, Texas. Journal of Geophysical Research 113, D17315.

Rubio, M.A., Oyola, P., Gramsch, E., Lissi, E., Pizarrod, J., Villena, G., 2004. Ozone and peroxyacetylnitrate in downtown Santiago, Chile. Atmospheric Environment 38, 4931–4939.

Rutllant, J., Garreaud, R., 1995. Meteorological air pollution potential for Santiago, Chile: towards an objective episode forecasting. Environmental Monitoring and Assessment 34, 223–244.

Rutllant, J., Garreaud, R., 2004. Episodes of strong flow down the western slope of the subtropical Andes. Monthly Weather Review 132, 611–622.

Sanhueza, P.A., Reed, G.D., Davis, W.T., Miller, T.L., 2003. An environmental decision-making tool for evaluating ground-level ozone-related health effects. Journal of the Air and Waste Management Association 53, 1448–1459.

Sardeshmukh, P.D., Hoskins, B.J., 1988. The generation of global rotational flow by steady idealized tropical divergence. Journal of the Atmospheric Environment 45, 1228–1251.

Schmitz, R., 2005. Modeling of air pollution dispersion in Santiago de Chile. Atmospheric Environment 39, 2035–2047.

Villena, G., Kleffmann, J., Kurtenbach, R., Wiesen, P., Lissi, E., Rubio, M., Croxatto, G., Rappenglück, B., 2011. Vertical gradients of HONO, NO*x* and O3 in Santiago de Chile. Atmospheric Environment 45, 3867–3873.

Wang, B., 2011. Multi-model ensemble forecast of MJO: progress of ISV Hindcast Experiment (ISVHE) and preliminary results. Climate Test Bed PI's Meeting, 06 Oct 2011, Fort Worth, TX, A3.

Wheeler, M.C., Hendon, H.H., 2004. An all-season real-time multivariate MJO index: development of an index for monitoring and prediction. Monthly Weather Review 132, 1917–1932.

Zhang, C., 2005. Madden–Julian oscillation. Geophysics 43, 1–36.